Design and Experiment of 340-GHz Band Pass Filter With Low Insertion Loss

NAIBO ZHANG [1,2], **RUILIANG SONG**[1], **CHUNTING WANG**[1],
MINGJUN HU[3], **QIUQUAN GUO**[4], **AND JUN YANG**[4]

[1]54th Research Institute, China Electronics Technology Group Corporation, Beijing 100070, China
[2]Beijing University of Posts and Telecommunications, Beijing 100876, China
[3]Beihang University, Beijing 100191, China
[4]Department of Mechanical and Materials Engineering and Biomedical Engineering Program, Faculty of Engineering, Western University,
London, ON N6A 3K7, Canada

Corresponding authors: Naibo Zhang (zhangnaibai@163.com) and Qiuquan Guo (qguo29@uwo.ca)

ABSTRACT This paper demonstrates a 340-GHz band pass filter with a low insertion loss of ~-0.6 dB and a bandwidth of $\sim$6%. This paper studies the relationship between filter diaphragm thickness and resonator length, and the quantitative relationship between insertion loss and fabrication tolerances. The diaphragm is quantitatively analyzed and the resonators lengths with correction factors are calculated for the accurate and robust filter parameters, and the simulation results based on calculated parameters show a robust filter structure as well as a good agreement with the theoretical analysis. The surface roughness and filter structure sizes deviation with different tolerances are studied and calculated for insertion loss. Finally, a filter with low insertion loss and good robustness is achieved by calculated parameters and a certain fabrication tolerance. Different fabrication precisions are carried out to verify the effect of size tolerances on the filter performance, including insertion loss and structural robustness. The filters, designed by the parameters analysis and fabricated by $\leq \sim 7.5$-μm accuracy show good agreement between the simulation results and the test results, and when fabricated accuracy is $\sim$5 μm, the insertion loss is ~-0.6 dB and the return loss is < -20 dB.

INDEX TERMS Band pass, filter, WR2.8.

I. INTRODUCTION

There is a growing interest in terahertz components in the frequency from 300 GHz to 10 THz for potential applications in security scanning, atmospheric monitoring, medical imaging and ultrafast wireless communications [1]. Developing terahertz components with high performance is essential in manipulating terahertz waves with well-defined characteristics [2]. In general, design and fabrication are widely studied for terahertz filters. In design methods, these techniques can be roughly divided into three categories: waveguide structure [1], [3]–[8], meta-material structure [2], and frequency selected surface (FSS) [9]–[12]. Due to the advantages of low transmission loss, high power capacity, and suitability for fabrication by the micromachining process, rectangular waveguide structures are widely used for terahertz application [13], in conventional design method, however, the fabrication accuracy limits to further higher frequencies of filters. Meta material structure filter and

frequency selected surface (FSS) filters are good candidates of terahertz filter, which exhibit insertion loss <1 dB at 700 GHz under experimental measurement [11], [12]. However, due to the simple resonant structure, the stopband rejection of mesh filter is imperfect, and hard to integrate with waveguide module, sensitive to installation and environment. Many different fabrication technologies have been reported in literature, among them three categories have been found: SU8 photoresist-based processes [1], [14], LIGA [5], MEMS (DIRE and ICP) [8]–[10], [14], [15] and CNC milling [3], [4], [6]. Photolithographic based micromachining technology has attracted growing attention due to its high-dimensional accuracy. For instance, SU8 photoresist technology [16], [17] affords good dimensional accuracy and at the same time with low capital investment required. MEMS technology provides a high-dimensional accuracy, high achievable structure aspect ratio and capability of large scale inexpensive production, however, the insertion loss of this type filter is not perfect (~-10 dB [9], and ~-3.5 dB [12]) because of the limitation of structure design and quality factor (Q). In addition, parameters matchings and

---

The associate editor coordinating the review of this manuscript and approving it for publication was Feng Lin.

robustness of parameters are the other main factor affecting the insertion loss. In [3], [4], [7], [22], and [23], the structures are designed based on H ladder rectangle waveguide, and the parameters are obtained by equivalent circuit and structural optimization simulation, however, some key parameters have not been well analyzed and calculated, for instance, in [4], the diaphragm thickness is simply estimated without accurate calculation. And the robustness of parameters [3], [4], [12] has not been analyzed, which directly affects the insertion loss of the filter when the low fabrication tolerance occurs.

This paper mainly discusses from two aspects: 1) Terahertz filter parameters calculation, the resonators lengths with correction factors were introduced into filter structure calculation, parameters matching and return loss (low insertion loss) in pass band were analyzed, and simulations were carried out to verify the analysis. 2) Insertion loss analysis, the quality factor (Q) and sizes tolerances are discussed and analyzed, different fabrication accuracy is used to verify the analysis results, and it is obtained that the insertion loss is mainly caused by surface roughness and filter structures sizes deviation.

II. FILTER PARAMETERS CALCULATION

Rectangular waveguide filter design is mature, this section does not repeat the design method. In this section, the traditional design method is cited, and this part focuses on the calculation method of diaphragm thickness, the calculation of diaphragm thickness and resonance length. The diaphragm thickness t ($100 \sim 1000 \ \mu m$) of conventional H-ladder waveguide filter structure (center frequency <30 GHz) has little influence on the filter performances. However, when the frequency is up to 300 GHz, the diaphragm thickness ($\sim 50 \ \mu m$) has great influence on the filter performances. Moreover, the variation of diaphragm thickness (t) can lead to changes in other parameters (x and P). In order to obtain the accurate parameters (t, x and P) and good performances, the detailed analysis is provided as following.
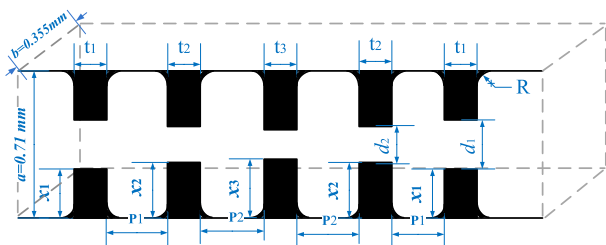

FIGURE 1. Side view of bandpass filter.

A. THEORETICAL ANALYSIS

Fig.1 shows the filter structures, the rectangular waveguide (WR2.8) was used for the filter, the parameters are shown in Fig.1. Fig.2(a) is the equivalent circuit, which was used for analyzing the relationship between the voltage standing wave ratio (VSWR) and reactance in the reactance discontinuity point, the diaphragm is jB_i. The diaphragm is equivalent to the circuit as Fig.2(b), the relationship between
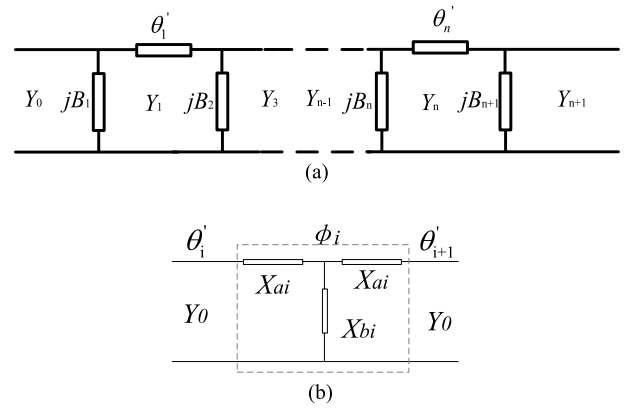

FIGURE 2. (a) Traditional reactance coupling circuit diagram. (b) Equivalent circuit of diaphragm thickness [25].

X_{ai}/X_{bi} and S parameters is deduced by $ABCD$ matrix, where Y_0 is admittance of waveguide.

$$X_{ai} = \frac{1}{Y_0} \left(\frac{1 - S_{21} + S_{11}}{1 - S_{11} + S_{21}} \right) \tag{1}$$

$$X_{bi} = \frac{1}{Y_0} \left(\frac{2S_{21}}{1 - 2S_{11} + S_{11}^2 - S_{21}^2} \right) \tag{2}$$

The electric length (ϕ_i) of diaphragm thickness (t) is expressed as [25],

$$\phi_i = -\arctan(2Y_0 X_{bi} + Y_0 X_{ai}) - \arctan(Y_0 X_{ai}) \tag{3}$$

The electric length (θ_i') of resonator length (P) is expressed as,

$$\begin{aligned}
\theta_i' &= \frac{\pi}{2} + \varphi_i' + \varphi_{i+1} \\
&= \frac{\pi}{2} + \frac{1}{2} \left[\arctan \sqrt{\rho_i}/2 - \frac{1}{2\sqrt{\rho_i}} + \arctan \sqrt{\rho_{i+1}}/2 \right. \\
&\quad \left. - \frac{1}{2\sqrt{\rho_{i+1}}} \right]
\end{aligned} \tag{4}$$

where, ρ is standing-wave ratio (SWR). Because the diaphragm (t) is about 30-100 μm, it can't be ignored in THz band, the actual electric length (θ_i) of resonator is,

$$\theta_i = \theta_i' + \Delta_i \cdot \phi_i + \Delta_{i+1} \cdot \phi_{i+1} \tag{5}$$

The equivalent resonators length l_1 and l_2 are expressed as,

$$\begin{aligned}
l_1 &= P_1 + \Delta_1 \cdot t_1 + \Delta_2 \cdot t_2 \\
l_2 &= P_2 + \Delta_2 \cdot t_2 + \Delta_3 \cdot t_3
\end{aligned} \tag{6}$$

where, Δ_1, Δ_2 and Δ_3 are correction factors. Because the diaphragm (t) has great influence on the performance of the filter, the parameter t can't be directly used as the resonance length, which needs to be corrected. Parameters t_1, t_2 and t_3 are defined as 40 μm, 60 μm and 40 μm, respectively.

When diaphragm thickness (t) and gap width ($d_i = a - 2x_i$) change, the bandwidth (BW), center frequency (f_0) and the coupling coefficient ($k_{i,i+1}$) change accordingly.

$$k_{i,i+1} = \frac{BW}{f_0 \sqrt{g_i g_{i+1}}} \tag{7}$$

where, g_i is the parameter of the Chebyshev low pass prototype filter. The diaphragm sizes (t, $d_i = a - 2x_i$) effect the coupling coefficient ($k_{i,i+1}$) which leads to filter performance changes. When $\Delta_i \cdot t_i$ is reduced, the coupling coefficient among resonators decreases, and d_i is increased to balance the coupling coefficient. So, $\Delta_i \cdot t_i$ and d_i have an inverse relationship.

$$\Delta_1 \cdot t_1 \cdot d_1 = C_1, \Delta_2 \cdot t_2 \cdot d_2 = C_2, \Delta_3 \cdot t_3 \cdot d_3 = C_3 \quad (8)$$

To ensure that there is no reflection in the passband, C_1, C_2 and C_3 are defined as constants, after that, it is defined that $P_1 = 0.44$ *mm*. According to equations (4)-(6), (8), and (23)-(31), the parameters can be calculated as, $\Delta_1 = 3.54$, $\Delta_2 = 2.96$, $\Delta_3 = 5.54$, $P_2 = 0.492$ *mm*, $x_1 = 0.17$ *mm*, $x_2 = 0.22$ *mm*, $x_3 = 0.24$ *mm*.

B. SIMULATIONS ANALYSIS

In order to verify the analysis above, the simulations are carried out. The details are as following: the relative bandwidth (*BW*) is designed as 6%, the attenuation is ~ 35dB when the frequency equals to $f_0 \cdot (1 \pm 10\%)$, where f_0 is the center frequency (340GHz), the VSWR in passband is designed as 1.02, and four orders resonators were used for the filter. The wavelength of rectangular waveguide (λ_g) is 1.27 *mm*, $\lambda_0 = 0.882$ *mm* and $a = 710$ μm. According to analysis (In section "Appendix"), $(B_i/Y_0) \cdot (a/\lambda_g)$ is about 1.09, 4.41 and 9.84, where i equals to 1, 2, and 3, respectively. And according to [22], the d_i/a are about 0.51, 0.38 and 0.32, respectively. So $d_1 = d_5 = 0.36mm$, $d_2 = d_4 = 0.27$ *mm*, $d_3 = 0.23$ *mm*, where, $d_i = a - 2x_i$. The parameters can be calculated as, $\Delta_1 = 3.54$, $\Delta_2 = 2.96$, $\Delta_3 = 5.54$, $P_2 = 0.492$ *mm*, $x_1 = 0.17$ *mm*, $x_2 = 0.22$ *mm*, $x_3 = 0.24$ *mm*. In addition, in order to verify the effect of size tolerances on the performance, the structure is simulated by increasing or decreasing the parameters based on the calculated parameters. All simulations are carried out by Ansoft *HFSS*.
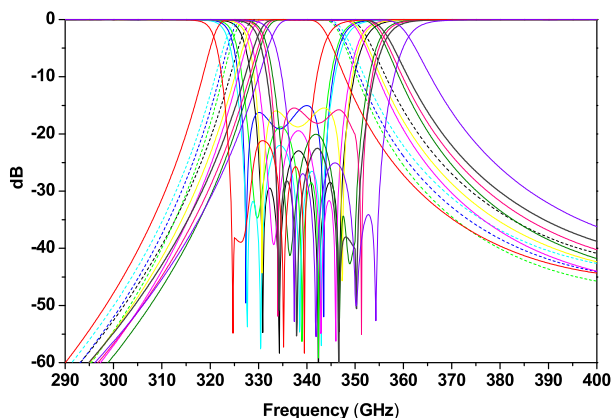
FIGURE 3. RF performance of the filter.

Fig.3 shows the RF performances of filters, the parameters and performances details are shown in the TABLE 1. All structure parameters in the TABLE 1 show the performances with insertion loss of <0.2dB and return loss of > 16dB.

TABLE 1. Parameter and performance details of filters.

| Filters	Width of beam (mm)		Length of resonator (mm)		RF performance (GHz, GHz, dB, dB)			
	t_1	t_2	P_1	P_2	f_0	BW	S_{21}	S_{11}
1	0.04	0.06	0.46	0.52	330	16	< 0.1	>20
2	0.04	0.06	0.45	0.51	335	20	< 0.1	>20
3	0.04	0.06	0.44	0.5	339	20	< 0.1	>22
4	0.04	0.06	0.43	0.49	340	22	< 0.1	>22
5	0.04	0.06	0.42	0.48	346	22	< 0.1	>20
6	0.04	0.07	0.45	0.51	337	20	< 0.2	>16
7	0.04	0.07	0.44	0.5	339	18	< 0.2	>16
8	0.04	0.07	0.43	0.49	342	20	< 0.2	>16
9	0.05	0.07	0.45	0.51	335	18	< 0.2	>16
10	0.05	0.07	0.44	0.5	339	18	< 0.15	>18
11	0.05	0.07	0.43	0.49	341	18	< 0.15	>18
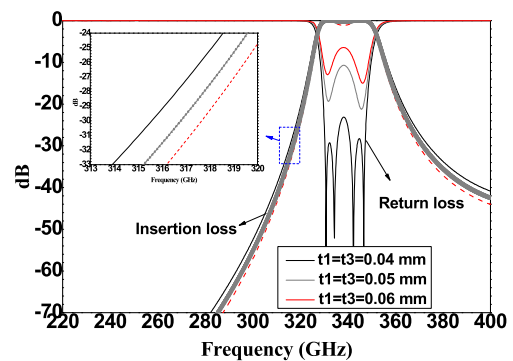
FIGURE 4. RF performances of filter when t_1 and t_3 changes from 0.04 *mm* to 0.06 *mm*.

From the first five groups data, when the P_1 and P_2 are changed by a step of 10 μm, the return loss is >20dB and insertion loss <0.1dB in pass band. From the last six groups data, when the thickness of the diaphragm (t) is changed by a step of 10 μm, the insertion loss is >16dB and insertion loss <0.2dB in pass band. From data groups in the table (4th and 8th, 4th and 11th, 8th and 11th, 2th and 10th), the diaphragm thickness (t) has a great impact on f_0, BW(bandwidth), S_{21} and S_{11}. We used to study the influence of parameter t on the performance in previous works, different thicknesses (t) are simulated. When $t_2 = 0.06mm$, $P_1 = 0.44$ *mm*, $P_2 = 0.44$ *mm*, $P_2 = 0.5$ *mm* (optimized by HFSS), and $t_1(= t_3)$ changes from 0.04 *mm* to 0.06 *mm*, the performances are shown in Fig.4. When t_1 and t_3 increased, the performances (S_{11}/S_{21}) deterioration, but f_0 and BW (bandwidth) keep constant.

When $t_1 = 0.04$ *mm*, $P_1 = 0.44$ *mm*, $P_2 = 0.5$ *mm*, t_2 changes from 0.04 *mm* to 0.06 *mm*, the simulation results are shown in Fig.5. In the figure, when t_2 increased, the performance (S_{11}/S_{21}) is better than before, and the f_0 and BW (bandwidth) keep constant. The diaphragm thickness (t) affects the S_{21} and S_{11}, but has no effect on the BW and f_0. The fillet parameter (R) has certain influence on performances as well. When R changes from 10 μm to 50 μm, f_0 increased, BW decreased. When R increased, f_0 and BW increased, vice versa. The simulation results were shown in Fig.6. However, the fillet just has a little influence on performance
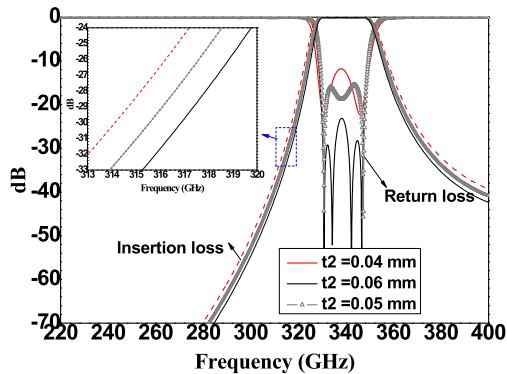
FIGURE 5. RF performances of filter when t_2 changes from 0.04 *mm* to 0.06 *mm*.
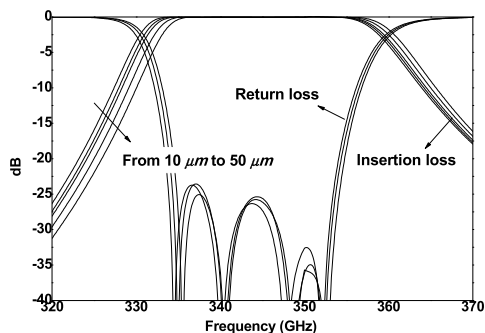

FIGURE 6. RF performance in different fillet size.

of insertion loss, so the fillet can be used for fine-turning f_0 and BW of the filter.

In summary, the diaphragm thickness (t) is used to optimize the parameters S_{21}/S_{11}, and the parameter R is used to optimize the parameters f_0 and BW. In addition, in order to obtain low insertion loss and high return loss in the actual situation, besides the above analysis, the parameters matching and resistance loss of the cavity surface need to be studied. This part will be studied in detail in next section.

III. INSERTION LOSS ANALYSIS

When the filter structure parameters are determined, there are two main factors determining insertion loss, quality factor (Q) and filter structures sizes deviation. The quality factor (Q) is determined by surface roughness. The insertion loss is determined by following factors.

a) The insertion loss of ripple is expressed as.

$$L_{Ar} = 10 \log \left[1 + \frac{(\rho_r - 1)^2}{4\rho_r} \right] \qquad (9)$$

where, ρ_r is the VSWR of ripple in pass band. The max $\rho_r = r \ Z_i/Z_o$, which is the impedance ratio of the input to output. Because the filter structure is symmetric, ρ_r is defined as ~1.25 [22], the max insertion loss in pass band is ~0.065dB. The insertion loss of ripple can be ignored in this paper.

b) The insertion loss caused by quality factor (Q).

The quality factor (Q) is caused by surface roughness which is produced by fabrication accuracy. The unloaded

quality factor Q_u [25], [26] is determined by Q_c (A lossy conductor wall, but a lossless medium filled with the cavity) and Q_{fab} (Caused by fabrication factors, such as metal stroke quality, thickness and roughness) [25],

$$\frac{1}{Q_u} = \frac{1}{Q_c} + \frac{1}{Q_{fab}} \qquad (10)$$

where,

$$Q_c = \frac{(kal)^3 b\eta}{2\pi R_s} \frac{1}{(2a^3b + 2bl^3 + a^3l + al^3)}$$
$$R_s = \sqrt{w\mu_0/(2\sigma)}$$
$$Q_{fab} = w \frac{\mu_0 \int_V |H|^2 \, dV}{\sigma \int_S |H_t|^2 \, dS}$$

And a, b and l are length, width and height of the cavity, k is propagation constant, η is wave impedance, σ is conductivity (=41,000,000 S/m), R_s is surface resistance of metal wall in waveguide, w is frequency, and μ_0 is vacuum permeability, H is space magnetic field, H_t is spatial transverse magnetic field, S is inner surface of space, and V is volume in space.
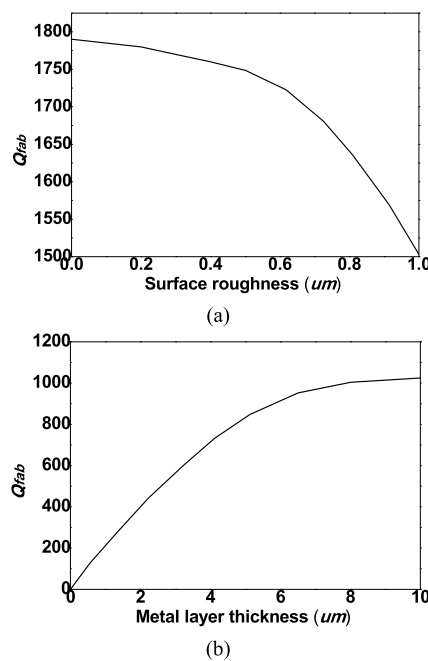

FIGURE 7. (a) The relationship between surface roughness and Q_{fab}. (b) The relationship between metal thickness and Q_{fab}.

The insertion loss that mainly caused by Q_{fab} is determined by surface roughness and metal layer thickness [12]. Fig.7 shows the relationship between surface roughness/metal layer thickness and Q_{fab}. When metal layer thickness is infinity, Q_{fab} decreases with the increase of roughness, when the roughness is greater than 0.7 μm, Q_{fab} drops sharply. When surface roughness is zero, Q_{fab} increases with the increase of metal layer thickness, when the roughness is greater than 7 μm, Q_{fab} is almost up to the maximum.
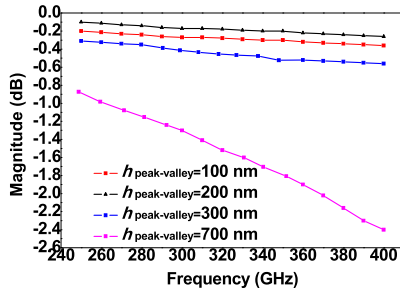
FIGURE 8. The effect of the surface roughness to the insertion loss. Gold layer thickness is 2.5 μm, d_{peak} is set as 9.4 μm, and the length is 22.12 mm.
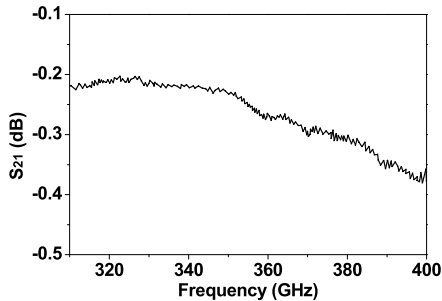

FIGURE 9. Measurement of 22.12 mm long rectangular waveguide prototype for the WR-2.8 band.

Gold layer ($\sim$ 2.5 μm) is electroplated on the filter surface, however, the surface roughness still exits inside the waveguide and has an impact on the insertion loss. In this paper, the Huray model is chosen to simulate the roughness of the gold layer [12], [24]. The conductivity of electroplated gold film (3.96 X 10^7S/m) is less than gold bulk [19]. The height between peak and valley in the surface is $h_{peak-valley}$, and the max distance between adjacent peaks is d_{peak}. In this paper, the d_{peak} is set as 9.4 μm [24], and $h_{peak-valley}$ ranges from 100 nm to 700 nm, and the length of the waveguide is 22.12 mm. Fig.8 shows the relationship between the surface roughness and the insertion loss when metal layer thickness is $\sim$ 2.5 μm. The work in [12], [24], and [19] also uses this model to analyze the loss. Another approach to analyze the surface roughness is using the equivalent conductivity which includes the effect of roughness. Fig.9 shows the insertion loss measurement of rectangular waveguide prototype for the WR-2.8 band with 22.12 mm long, the fabrication tolerance is $\sim$5 μm, the gold layer is $\sim$2.5 μm. The insertion loss is $\sim$−0.22 dB at 340 GHz, and >−0.4 dB from 320 GHz to 400 GHz, the test results coincide with the analysis.

c) The insertion loss caused by filter structures sizes deviation.

The deviation of the filter structure size is caused fabrication tolerance. When the quality factor (Q) is determined, the parameters matching is the main factor for the insertion loss. When parameters are determined as:$x_1 = 0.17$ mm, $x_2 = 0.22$ mm, $x_3 = 0.24$ mm, $\Delta_1 = 1.77$, $\Delta_2 = 1.48$, $\Delta_3 = 2.77$, P$_2 = 0.492$ mm. The CNC fabrication has a characteristic: when one parameter tolerance is ±5 μm,

TABLE 2. Insertion loss caused by different fabrication tolerances.

Fabrication tolerance (μm)	1	2	4	5	6	7	10	16	20
Insertion loss ($\sim$ dB)	0.1	0.2	0.35	0.4	0.5	0.6	1.2	3	3.7

the other parameters tolerances are all ±5 μm, which means all parameters increased/decreased $\sim$5 μm at the same time. According to the characteristics, different fabrication tolerances are calculated and simulated. TABLE 2 shows the simulation results with fabrication tolerances. Here we try to construct the insertion loss (y) function that caused by fabrication tolerance (x). This function should satisfy the following conditions: 1) This function is monotonically increasing, i.e., y increases with x. 2) But it is not a uniform process between x and y, that is, derivation of y is not a constant. 3) When x is a small value and changes very little, y increases little, when x reaches a certain value, y increases rapidly, where the x value has a certain range, and then the change characteristics of the exponential function meet the above conditions, we define the following functions.

$$y = Ae^{g(x)} + B \tag{11}$$

is the variation between x and y strictly consistent with the exponential function here? Obviously, the probability is small, because the relationship between x and y is monotonically increasing, and $x > 0$, we simplify the construction of a function for analysis.

$$g(x) = a(x + b)^n + c \tag{12}$$

When $x \in (x_1, x_2)$, The derivation of $y(x)$ can be obtained.

$$y'(x) = Aan(n + b)^{n-1}e^{g(x)} \tag{13}$$

For different structure filters and different parameter values, the $y(x)$ derivative values can be used to illustrate the robustness of the filter. The smaller the value, the better the robustness. In this paper, the fabrication tolerance is simulated by increasing or decreasing the sizes of the filter structures, and the simulation curves of different fabrication tolerances are obtained by electromagnetic simulation. Because the $y(x)$ function contains six parameters, six mathematical equations can be established by six sets of simulation curves, and the six sets data are chosen from TABLE 2, thus the insertion loss function caused by the tolerances of the filter structures can be obtained. The specific function form is shown below.

$$y = 1.68e^{\frac{x-3.71}{14.7}} - 1.36 \tag{14}$$

From Fig.8 and equation (14), if ±5 μm fabrication precision was used and when fabrication tolerances are <5 μm, the filter performance changes are not sensitive, and when fabrication tolerances is > $\sim$±6 μm, this effect on S_{21} is beginning to become sensitive.

In order to further verify the relationship between all dimensional deviations and insertion loss, Fig.11 shows the filter simulation results in different fabrication tolerances
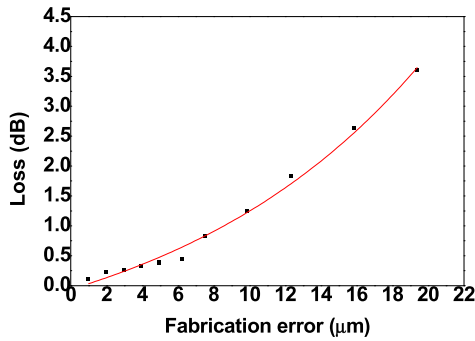
FIGURE 10. The relationship between fabrication tolerance and filter insertion loss in pass band.
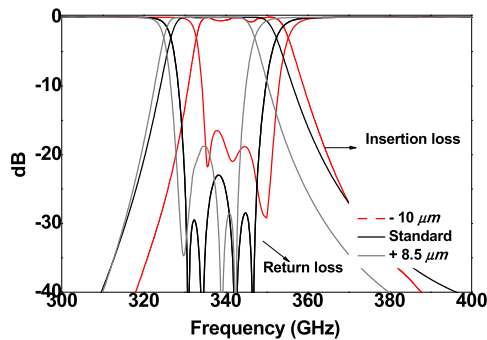

FIGURE 11. RF performance of the filter in different tolerances.

with no surface roughness, when there are no fabrication tolerances, the performance is the red curve in the figure, the insertion loss is > -0.1dB, and return loss is $\sim < -25$dB. When fabrication tolerances are 8.5 μm, the return loss is < -18 dB, and insertion loss is > -0.75dB, when fabrication tolerances is 12 μm, the return loss is < -14 dB, and insertion loss is ~ -2 dB. And these results validate the results of the above analysis.

Because there are two main factors that determine the insertion loss of filter: 1) fabrication factors: Q value caused by fabrication, and dimension error caused by fabrication, 2) filter structure parameters, matching relationship between design parameters (S_{11} value). When the fabrication tolerance is determined, If the insertion loss of the filter ($|S_{21}|$) is to be reduced, only the filter parameters can be reasonably designed to make S_{11} small enough. For instance, when S_{11} is less than -20 dB, the insertion loss ($|S_{21}|$) will be small enough, and if S_{11} is greater than -10 dB, the insertion loss ($|S_{21}|$) will be larger.

Section II.A provides parameters calculation method. The filter parameters obtained from the above calculation method can make the parameters match in the required frequency band, so as to ensure more energy passing through without reflecting back, making S_{11} smaller, and thus obtaining lower return loss (S_{11}). In this way, a lower insertion loss ($|S_{21}|$) can be obtained. However, to further reduce insertion loss ($|S21|$) on the basis of the above, it is necessary to modify the relationship between the parameters C_1, C_2 and C_3 and relationship between the parameters Δ_1, Δ_2 and Δ_3 in

Formula (6) and (8) to obtain smaller return loss (S11) and achieve lower insertion loss ($|S21|$).

IV. FABRICATION AND RESULTS ANALYSIS

In order to verify the insertion loss analysis in section III, three kinds of fabrication accuracy are selected for the filter, which are $\sim 5\mu m$, $\sim 7.5\mu m$ and ~ 15 μm respectively.

A. FABRICATION PROCESS AND MEASUREMENT SETUP

The high precision CNC milling process was used for filter fabrication, and copper blocks were utilized as substrate material. The WR-2.8 rectangular waveguide (0.71 $mm \times$ 0.355 mm) was used for the filter. Two half structures were bonded by screws, and the waveguide components are combined by two identical halves in E-plane. The CNC process with different fabrication accuracy was employed for filter fabrication. Two blocks copper with a thickness of 10 mm are chosen as the top and bottom substrates. The copper blocks are polished. After the structure models are established with detail parameters, the structures are fabricated by CNC process. Then the structure is electroplated with 2.5 μm gold. Next, two fabricated half structures are bonded together by pins and screws. Fig.11(a) show the filter structures, the flanges were designed and fabricated integrally, Fig.12(b) shows the fabricated filter.
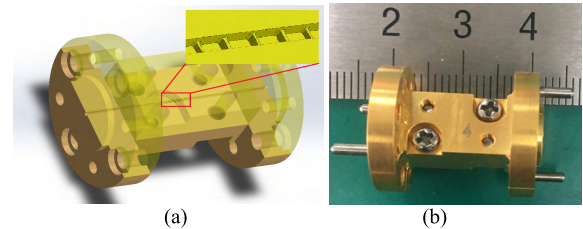

FIGURE 12. 340GHz filter appearance structure.

The measurement is carried out by Agilent vector network analyzer (VNA) av3672b, and control module is av3640a with two frequency extenders av3649. The trough-reflect-line (TRL) calibration is used during the measurement. The flanges (WR-2.8 UG-387/UM) on the extenders were used to connect the test fixture and fixed by screws, and the measurement setup connector is WR-2.8 waveguide.

B. MEASUREMENT RESULTS

In order to compare the difference among simulation results with no fabrication tolerance, simulation results with fabrication tolerances, and measurement results with different fabrication tolerances. The fabricated filters are shown in Fig.13, six filters were fabricated in different accuracy, which were used to verify the effect of accuracy. The fabrication accuracy in No. 1 is ~ 15 μm, No.2-4 is ~ -7.5 μm, No.5 is ~ 7.5 μm, and No. 6 is ~ 5 μm(test by metallurgical microscope). Because the consistency of CNC fabrication tolerances, when the fabrication tolerance is $\sim$ x μm, all fabricated structures will decrease x μm, and this feature will be used in simulations with x μm tolerances.
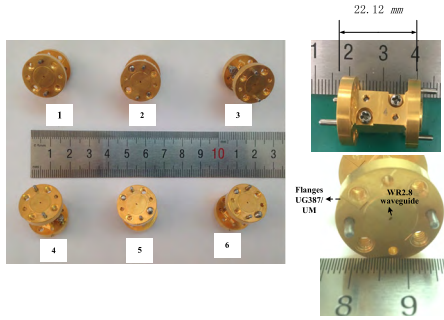
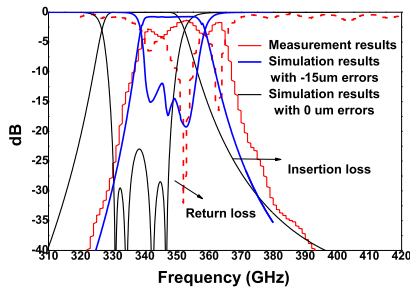**FIGURE 13.** Fabricated filter in different accuracy.

FIGURE 14. Measurement results in ~ −15 μm fabrication accuracy.

Fig.14 shows the comparison of measured and simulated results. The fabrication tolerance is ~ 15 μm, and the simulation result with 15 μm tolerances have an approximation agreement with measurement results. However, the thickness and spacing of diaphragm are smaller than simulation structures, and the matching between resonators is worse than simulations, the bandwidth becomes wider and the S_{21}/S_{11} becomes worse. The insertion loss in Fig.14 is caused by the parameters mismatching and surface roughness (~700 nm). According Fig.7-8, when fabrication tolerance is ~15 μm, ~2.5dB insertion loss is caused by parameters mismatching, and the remaining ~1.5dB (insertion loss) is mainly produced by surface roughness and test errors. Fig.15 shows three groups of performance, simulation results with no fabrication tolerances, simulation results with ~±7.5 μm, and measurement results. The measurements results show a good agreement with simulation results with ~±7.5 μm, and some differences with simulation results with no fabrication tolerances. The fabrication tolerances make the resonator unit size become smaller/bigger, which results in the center frequency increasing/decreasing. The insertion loss in Fig.15 is ~ 1.5 dB, including ~ 0.7 dB caused by parameters mismatching and ~ 0.8 dB mainly produced by surface roughness (~ 300 nm) and test errors. In Fig.16, the measurement results show a good agreement with two groups simulation results. The fabrication tolerance is ~ 5 μm tested by metallurgical microscope. The simulation with ~ 5 μm tolerances is carried out, which has a perfect coincidence with measurement results. Fig.16(b) shows the expanded view of S_{21}, which show ~−0.6 dB of measured result in passband. The insertion loss is ~0.6 dB, including ~ 0.4 dB caused by parameters mismatching, and ~ 0.2dB produced by surface
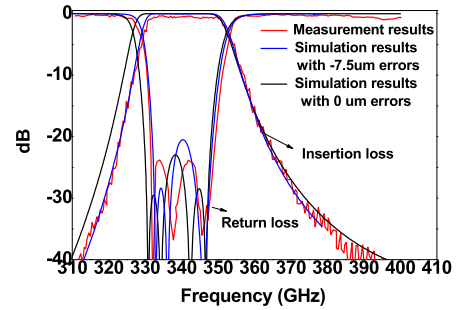
(a)
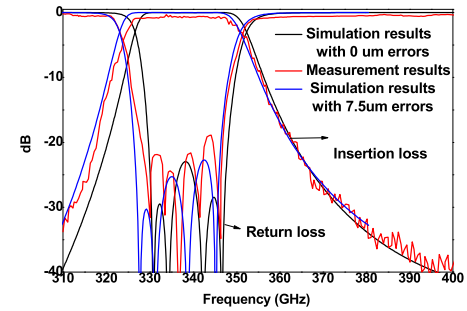
(b)

FIGURE 15. Measurement results in ~~ ± 7.5 μm fabrication accuracy. (a) ~−7.5 μm fabrication accuracy. (b) ~+7.5 μm fabrication accuracy.
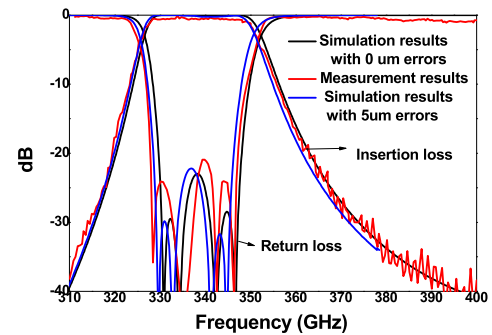
(a)
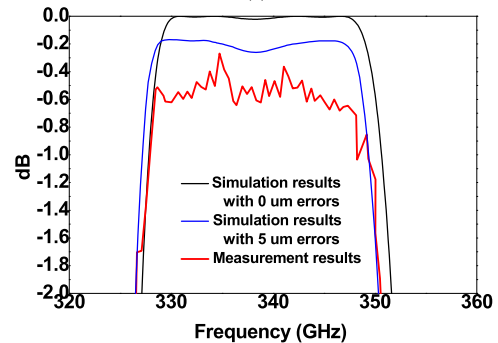
(b)

FIGURE 16. (a) Measurement results in ~ 5 μm fabrication accuracy. (b) Expanded view of S_{21}.

roughness (~ 200 nm) and test errors. Therefore, the RF performance differences is very small when the fabrication tolerances are 5 μm. In addition, the filter has a good insertion loss under this fabrication tolerances and good parameters matching design. The performance will not change greatly

under 5 μm fabrication tolerances. When the tolerances are larger than 7.5 μm, the performance will change greatly.

In order to compare the fabrication tolerances influence on the simulation results and test results, the simulation and measurement sizes of filter structures are shown in the table 3, the filter sizes are tested by metallurgical microscope, and the detail comparison of simulation and measurement results are shown in the table 4. It can be seen from the above measurement results that the influence of tolerances on performance is reflected in insertion loss, center frequency point and bandwidth. According to the test and simulation results, the total insertion loss of the filter is consistent with the analysis in section IV.

TABLE 3. Simulated and measured dimensions of filters.

Parameters sizes(μm) / Tolerances (μm)		t_1	t_2	x_1	x_2	P_1	P_2
0		40	60	170	220	440	500
5	Simu.	35	55	165	215	445	505
	Meas.	36.5	56	165.5	216	445.5	505.5
7.5	Simu.	32.5	52.5	162.5	212.5	447.5	492.5
	Meas.	32.6	52.5	162.6	212.5	447.3	492.5
-7.5	Simu.	47.5	67.5	177.5	227.5	432.5	492.5
	Meas.	47.8	67.5	177.5	227.8	432	492.5
-15	Simu.	55	75	185	235	425	485
	Meas.	55.5	75	186	236	424.5	485.5

TABLE 4. Comparison of simulation and measurement.

Performances / Tolerances (μm)		f_0 (GHz)	S_{21} in pass band (dB)	S_{21} in pass band (dB)	BW (GHz) @-3dB
Simulation with no tolerance		340	> -0.3	< -22	20
5 μm	Simu.	339.8	> -0.4	< -20	20
	Meas.	339.8	> -0.6	< -20	20
7.5 μm	Simu.	338.8	> -0.7	< -20	21.5
	Meas.	338.9	> -1.5	< -18.6	21
-7.5 μm	Simu.	341	> -0.7	< -20	18.5
	Meas.	341	> -1.5	< -20	18.5
-15 μm	Simu.	350	> -2	< -11	16
	Meas.	354	> -4	< -5	21

By comparing the above results, it can be found that: 1) the simulation results with quantitative simulation tolerances are almost identical with the test results with corresponding fabrication tolerances. 2) The insertion loss of the filter is mainly composed of the parameters mismatching and the surface roughness, which is basically consistent with the analysis results of Fig. 8 and Fig. 10.

C. DISCUSSION

When fabrication tolerances increased ($\sim$−5/−7.5/−15 μm), f_0 increases. The reason is that the scale of filter structures are too close to the tolerance. The reason of the change in bandwidth is as following: the *ABCD* matrix of the filter is used for S_{21}, two equivalent transmission line matrix is

expressed as,

$$A_1 = \begin{bmatrix} cos\theta_1 & j\frac{1}{Y_0}\sin\theta_1 \\ jY_0\sin\theta_1 & cos\theta_1 \end{bmatrix},$$

$$A_2 = \begin{bmatrix} cos\theta_2 & j\frac{1}{Y_0}\sin\theta_2 \\ jY_0\sin\theta_2 & cos\theta_2 \end{bmatrix} \quad (15)$$

And the total matrix is, $A = A_1 \cdot A_2 \cdot A_2 \cdot A_1$.

$$A = \begin{bmatrix} \cos 2(\theta_1 + \theta_2) & j\frac{2}{Y_0}\cos(\theta_1 + \theta_2)\sin(\theta_1 + \theta_2) \\ j2Y_0\cos(\theta_1 + \theta_2)\sin(\theta_1 + \theta_2) & \cos 2(\theta_1 + \theta_2) \end{bmatrix} \quad (16)$$

The insertion loss is expressed as equation (17), in order to obtain the −3 dB cut-off angular frequency (w_{cn}), the equation (17) equals to $1/\sqrt{2}$.

$$\begin{aligned} |S_{21}| &= \left| \frac{2}{A_{11} + A_{12} + A_{21} + A_{22}} \right| \\ &= \left| \frac{1}{j(Y_0 + 1/Y_0)\cos(\theta_1 + \theta_2)\sin(\theta_1 + \theta_2) + \cos 2(\theta_1 + \theta_2)} \right| \\ &= \frac{1}{\sqrt{\cos^2 2(\theta_1 + \theta_2) + (Y_0 + 1/Y_0)^2 \cos^2(\theta_1 + \theta_2)\sin^2(\theta_1 + \theta_2)}} \\ &= \frac{1}{\sqrt{2}} \end{aligned} \quad (17)$$

The equivalent electric length is expressed as (18)-(19), the equation (18) is calculated from (17).

$$\theta_1 + \theta_2 = 0.479\pi + 0.5n\pi, \quad n = 0, 1, 2, 3... \quad (18)$$

$$\theta_1 + \theta_2 = \frac{l}{2}\beta = \frac{l}{2c}w \quad (19)$$

where, c is the speed of light, and $l = 2(l_1 + l_2) = 2(P_1 + P_2 + \Delta_1 \cdot t_1 + \Delta_2 \cdot t_2 + \Delta_3 \cdot t_3)$. The −3 dB cut-off angular frequency (w_{cn}) is obtained from (18)-(19), and expressed as,

$$w_{cn} = \frac{(0.958 + n)c\pi}{l} \quad (20)$$

And the bandwidth is expressed as,

$$BW = w_{c1} - w_{c0} = \frac{c\pi}{l} \quad (21)$$

In order to further illustrate the impact of fabrication tolerances on BW, the drift rate (r) used to indicate the impact of the fabrication tolerance on BW, the equation is as following,

$$r = \frac{\frac{(0.958+n)c\pi}{l} - \frac{(0.958+n)c\pi}{l+\Delta l}}{\frac{(0.958+n)c\pi}{l}} = \frac{\Delta l}{l + \Delta l} \quad (22)$$

where, Δl is equivalent length tolerance. From the equation (22), when fabrication tolerance is negative, Δl is a positive number, and then the filter size (l) increase, according to (21), BW decreased, vice versa.

TABLE 5. Comparison of different types THz filters.

	Center Frequency (GHZ)	Relative Band width	Configuration	Bandpass S_{21} (dB)	Bandpass S_{11} (dB)	Length (mm)	Techniques employed
Ref.[1] (2012)	~ 300	~ 8 %	Wave guide	~ 2.2	> 15	14.97	SU8
Ref.[2] (2015)	Low pass filter From 400GHz to 1.1THz	___	Meta material	~ 2	___	___	MEMS
Ref.[3] (2014)	340	~ 6%	Wave guide	~ 2.5	~ 12	___	CNC milling, then gold plating
Ref.[4] (2014)	140	~ 8%	Wave guide	~ 1.5	~ 18	___	CNC milling, then gold plating
Ref.[5] (2011)	Low pass filter From 220GHz to 275GHz	___	Wave guide	~ 2.3	~ 13.5	23.88	KMPR based UV-LIGA
Ref.[6] (2009)	~ 245	___	Wave guide	~ 3.81	> 25	254	CNC milling, then gold plating
Ref.[7] (2003)	~ 165	~ 7 %	Wave guide	~ 3	~ 12	8	SU8
Ref.[8] (2011)	~ 235	~ 6.4 %	Wave guide	~ 2.3	~ 10	___	MEMS, Silicon based on DIRE
Ref.[9] (2012)	~ 480	~ 20 %	Frequency Selective Surfaces	~ 10	___	___	MEMS
Ref.[10] (2011)	325	~ 8%	Frequency Selective Surfaces	~ 1.75	___	___	MEMS
Ref.[11] (2010)	325	~ 11.75%	Frequency Selective Surfaces	< 1	___	___	MEMS
Ref.[12] (2015)	~ 390	~ 7.7%	Wave guide	~ 3.5	> 15	___	MEMS, Silicon based on DIRE
Ref.[13] (2009)	~ 280	~ 25%	A combination of photolithography and mechanical lapping	~ 3	~ 15	11.4	SU8
This work	**340**	**~6%**	**Wave guide**	**~ 0.6**	**> 20**	**22.12**	**CNC milling, then gold plating**

It is generally believed that diaphragm t is $(1/30) \cdot P$ or less [22], which has no effect on the structure. If the thickness is greater than that, the diaphragm t will affect the resonant frequency and RF performance. This study presents relationships among parameters t, d and P. However, the calculated parameters have some differences with the final simulation results, the reasons are as following: SWR is required small enough in a certain bandwidth range, and t is inversely proportional to d, in order to simplify the calculation, two assumptions ($C_1 = C_2 = C_3$, and equals to constant) are made for fine-tuning the filter structure. However, there are a little difference among C_1, C_2 and C_3, and the parameter P are used to fine-tune in simulation, so there are some differences.

In addition, we comment that various micromachining methods for realizing filters show higher insertion loss than the CNC-milled based demonstration they describe in the paper, which does not mean that the CNC process is superior to other methods or that the loss due to the CNC process is reduced, for example, in reference [3], CNC process with 5 μm fabrication tolerance was used for 340 GHz bandpass filter (bandwidth is 6%), however, the insertion loss is ~2.5 dB. There are two main factors determining insertion loss, quality factor (Q) and the structure robustness.

The Q value is determined by surface roughness. When the fabrication tolerance is determined, the insertion loss caused by Q is determined. According to Fig.8 and Fig.14-Fig.16, we can find that the structure robustness is determined by parameters matching. For instance, when fabrication tolerance is ~5 μm, the insertion loss caused by Q is ~0.2 dB, and caused by parameters mismatching is ~0.4 dB. When fabrication tolerance is ~15 μm, the insertion loss caused by Q is ~1.5 dB, and caused by parameters mismatching is 2.5~3 dB. Some of the high precision micro-machined filters do not have a good insertion loss, mainly because the structural parameters are not well calculated and coordinated.

To compare the proposed filter in this study and reported THz filters, Table 5 shows recently published THz waveguide filters, FFS filters, and mate material filters. The proposed filter serves as bandpass filters with a low insertion loss which is comparable to the filter's performances [3]–[20]. The proposed filter provides high Q and return loss in pass band that are competitive with those of filters [3]–[15]. In other words, the proposed filter can have both the advantages of a high-quality factor, a low insertion loss and high return loss of passband. It is observed that the previously published filters could not provide such filter

with low insertion loss, high return loss. Compare with the bandpass filters with the same center frequency, rectangle waveguide and CNC milling in [3], the filter in this study shows a much better performances than performances in [3]. When compare with [11] and [12] with almost same center frequency and band width, the differences are fabrication and filter structures, the proposed filter in this study shows a lower insertion loss and a higher return loss in pass band. These advantage features of proposed filter will be useful for many system applications, such as, communication system and microwave detection system.

V. CONCLUSION

This paper presents a 340GHz band pass filter with insertion loss of ~ -0.6dB and band width of $\sim 6\%$. The filter was designed based on a rectangle waveguide of WR2.8, and fabricated by computer numerical control (CNC) milling process. The diaphragm thickness is quantitatively analyzed to obtain the accurate filter parameters by equivalent circuit and diaphragm coupling, the simulation results based on calculated filter parameters show that diaphragm thickness has great influence on the filter performance. Meanwhile, the relationship between fabrication tolerance and insertion loss was studied and a quantitative mathematical model is given for the first time. Based on the above analysis, the filter parameters were obtained. Different fabrication accuracy, carried out from 5 μm to 15 μm, was used for validating the influence of different CNC fabrication accuracy on the performance of filters. The test results show a good agreement with the theoretical analysis and simulation results. The filter also shows an excellent performance when compared with other filters performance from the current literature reports.

APPENDIX

In Fig.2(a), the parameters are defined as,

$$h_i = \frac{Y_i}{Y_{i-1}}, u_i = \frac{B_i}{Y_{i-1}} \quad (23)$$

where, $B_i = -\frac{jX_{bi}}{2X_{ai}X_{bi}+1}$ where, B_i is the junction susceptance and produced by diaphragm parameters (t and x). Y_i is the characteristic wave admittances of the waveguide sections, and produced by resonator (P).

The reflection coefficient in the equivalent circuit is,

$$\Gamma_i = \frac{Y_L - Y_{i-1}}{Y_L + Y_{i-1}} = \frac{(h_i - 1)Y_{i-1} + jB_i}{(h_i + 1)Y_{i-1} + jB_i} = \frac{(h_i - 1) + ju_i}{(h_i + 1) + ju_i} \quad (24)$$

The formula can be expressed as,

$$\rho_i + \frac{1}{\rho_i} = \frac{1 + h_i^2 + u_i^2}{h_i} \quad (25)$$

In this study, we defined that all Y_i are all equal, so $h_i = 1$. There is a formula as following.

$$u_i = \sqrt{\rho_i + \frac{1}{\rho_i} - 2} = \sqrt{\rho_i} - \frac{1}{\sqrt{\rho_i}} \quad (26)$$

In order to calculate the electrical length of adjacent coupling reactance, the individual discontinuous reactance is analyzed from Fig.2(b). Fig.2(c) is the equivalent circuits of the H-ladder waveguide bandpass filter ($n = 4$), the resistance of the filter is ignored for better calculation, since the resistance of the waveguide is <0.1 Ω.

Because the discontinuity reflection coefficient is a pure imaginary number, the electrical length can be obtained by following equations,

$$\theta_i' = \frac{\pi}{2} + \varphi_i' + \varphi_{i+1}$$
$$= \frac{\pi}{2} + \frac{1}{2}(\arctan \frac{u_i}{2} + \arctan \frac{u_{i+1}}{2}) \quad (27)$$

The parameters P, t, and x in Fig.1 are determined by equations (23)-(27). The order impedance of every diaphragm can be checked in [22] as, $Z_0 = 1$ (Input), $Z_1 = 5.613$, $Z_2 = 0.0875$, $Z_3 = 27.2$, $Z_4 = 0.1817$, and $Z_5 = 1.02$ (Output) respectively. And then, the VSWR of every order diaphragm were,

$$\rho_1 = \rho_5 = Z_1/Z_0 = 5.613$$
$$\rho_2 = \rho_4 = Z_1/Z_2 = 64.15$$
$$\rho_3 = Z_3/Z_2 = 310.86 \quad (28)$$

According to equation (26), the parameter u_i can be expressed as,

$$u_1 = u_5 = B_1/Y_0 = B_5/Y_0 = 1.95$$
$$u_2 = u_4 == B_2/Y_0 = B_4/Y_0 = 7.88$$
$$u_3 = B_3/Y_0 = 17.57 \quad (29)$$

So, according to equation (27), the electrical length of resonators can be calculated as,

$$\theta_1 = 150.015(l_1 = 0.53mm)$$
$$\theta_2 = 169.63(l_2 = 0.598mm) \quad (30)$$

The wavelength of rectangular waveguide is expressed as,

$$\lambda_g = \frac{\lambda_0}{\sqrt{1 - (\frac{\lambda_0}{2a})^2}} = 1.27mm. \quad (31)$$

REFERENCES

[1] X. Shang, M. Ke, Y. Wang, and M. J. Lancaster, "WR-3 band waveguides and filters fabricated using SU8 photoresist micromachining technology," *IEEE Trans. THz Sci. Technol.*, vol. 2, no. 6, pp. 629–637, Nov. 2012.

[2] Z. Zhu *et al.* "A metamaterial-based terahertz low-pass filter with low insertion loss and sharp rejection," *IEEE Trans. THz Sci. Technol.*, vol. 3, no. 6, pp. 832–837, Nov. 2013.

[3] C. Wang *et al.*, "0.34-THz wireless link based on high-order modulation for future wireless local area network applications," *IEEE Trans. THz Sci. Technol.*, vol. 4, no. 1, pp. 75–85, Jan. 2014.

[4] W. Cheng, L. Bin, L. Jie, and D. Xianjin, "140 GHz waveguide H ladder bandpass filter," in *Proc. IEEE Int. Conf. Microw. Millim. Wave Technol.*, May 2012, pp. 1–4.

[5] J. R. Stanec and N. S. Barker, "Fabrication and integration of micromachined millimeter-wave circuits," *IEEE Microw. Wireless Compon. Lett.*, vol. 21, no. 8, pp. 409–411, Aug. 2011.

[6] A. R. Kerr, C. Litton, G. Petencin, D. Koller, and M. Shannon, "Loss of gold plated waveguides at 210–280 GHz," Nat. Radio Astron. Observatory, Charlottesville, VA, USA, Tech. Rep., 2009.

[7] W. H. Chow, A. Champion, and D. P. Steenson, "Measurements to 320 GHz of millimetre-wave waveguide components made by high precision and economic micro-machining techniques," in *Proc. IEEE High Freq. Postgraduate Student Colloq.*, Sep. 2003, pp. 90–93.

[8] M. Vahidpour and K. Sarabandi, "Micromachined J-band rectangular waveguide filter," in *Proc. IEEE URSI Gen. Assem. Sci. Symp.*, pp. 1–4, Aug. 2011.

[9] S. Vegesna, Y. Zhu, A. Bernussi, and M. Saed, "Terahertz two-layer frequency selective surfaces with improved transmission characteristics," *IEEE Trans. THz. Sci. Technol.*, vol. 2, no. 4, pp. 441–448, Jul. 2012.

[10] R. Dickie, R. Cahill, V. Fusco, H. S. Gamble, and N. Mitchell, "THz frequency selective surface filters for earth observation remote sensing instruments," *IEEE Trans. THz. Sci. Technol.*, vol. 1, no. 2, pp. 450–461, Nov. 2011.

[11] M. Euler, V. Fusco, R. Cahill, and R. Dickie, "325 GHz single layer sub-millimeter wave FSS based split slot ring linear to circular polarization convertor," *IEEE Trans. Antennas Propag.*, vol. 58, no. 7, pp. 2457–2459, Jul. 2010.

[12] J.-X. Zhuang, Z.-C. Hao, and W. Hong, "Silicon micromachined terahertz bandpass filter with elliptic cavities," *IEEE Trans. THz Sci. Technol.*, vol. 5, no. 6, pp. 1040–1047, Nov. 2015.

[13] C. H. Smith, A. Sklavunuos, and N. S. Barker, "SU-8 micromachining of millimeter and submillimeter waveguide circuits," in *IEEE MTT-S Int. Microw. Symp. Dig.*, Jun. 2009, pp. 961–964.

[14] N. Zhang, Z. Deng, and F. Sen, "CPW tunable band-stop filter using hybrid resonator and employing RF MEMS capacitors," *IEEE Trans. Electron Devices*, vol. 60, no. 8, pp. 2648–2655, Aug. 2013.

[15] T. J. Reck, C. Jung-Kubiak, J. Gill, and G. Chattopadhyay, "Measurement of silicon micromachined waveguide components at 500–750 GHz," *IEEE Trans. THz Sci. Technol.*, vol. 4, no. 1, pp. 33–38, Jan. 2014.

[16] J. Carlier *et al.*, "Integrated microfluidics based on multi-layered SU-8 for mass spectrometry analysis," *J. Micromech. Microeng.*, vol. 14, pp. 619–624, Feb. 2004.

[17] A. Mata, A. J. Fleischman, and S. Roy, "Fabrication of multi-layer SU-8 microstructures," *J. Micromech. Microeng.*, vol. 16, pp. 276–284, Jan. 2006.

[18] M. Vahidpour and K. Sarabandi, "Micromachined J-band rectangular waveguide filter," in *Proc. IEEE URSI Gen. Assem. Sci. Symp.*, pp. 1–4, Aug. 2011.

[19] J. Hu, S. Xie, and Y. Zhang, "Micromachined terahertz rectangular waveguide band pass filter on silicon-substrate," *IEEE Microw. Wireless Compon. Lett.*, vol. 22, no. 12, pp. 636–638, Dec. 2012.

[20] Y. Li, P. L. Kirby, O. Offranc, and J. Papapolymerou, "Silicon micromachined -band hybrid coupler and power divider using DRIE technique," *IEEE Microw. Wireless Compon. Lett.*, vol. 18, no. 1, pp. 22–24, Jan. 2008.

[21] H. J. Tang, W. Hong, G. Q. Yang, and J. X. Chen, "Silicon based THz antenna and filter with MEMS process," in *Proc. IEEE Int. Workshop Antenna Technol*, pp. 148–151, Mar. 2011.

[22] B. Gan and W. Wu, *The Structure and Design of Modern Microwave Filter*. Beijing, China: Science Press, 1974.

[23] Z. Xing-Hai *et al.*, "MEMS rectangular waveguide filter at 140 GHz," *J. Infr. Millim. Waves*, vol. 32, no. 2, pp. 165–169, Apr. 2013.

[24] S. H. Hall *et al.*, "Multi-GHz, causal transmission line modeling methodology with a hemispherical surface roughness approach," *IEEE Trans. Microw. Theory Techn.*, vol. 55, no. 12, pp. 2614–2624, Dec. 2007.

[25] D. Yijia, B. Jing-Fu, Z. Xinghai, and Z. Yingbin, "Terahertz micromahcined waveguide filter," *J. Electron. Inf. Technol.*, vol. 34, no. 3, pp. 728–732, Mar. 2012.

[26] M. D. Pozar, *Microwave Engineering*, 3rd ed. New York, NY, USA: Wiley, 2005, pp. 280–281.
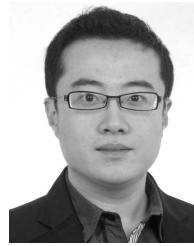
RUILIANG SONG received the B.E. and Ph.D. degrees in microelectronics and solid-state electronics from Tianjin University, Tianjin, China, in 2006 and 2009, respectively. From 2009 to 2011, he was a Postdoctoral Research Fellow with the Laboratory of CIGS Thin Film Solar Cells, Institute of Optoelectronic Thin Film Devices and Technology, Nankai University, Tianjin. Since 2011, he has been a Senior Engineer with the Beijing Research and Development Center, the 54th Research Institute, China Electronics Technology Group Corporation, Beijing, China. His current research interests include space terahertz communication systems, terahertz devices, and components in III-V compound semiconductors.

CHUNTING WANG received the Ph.D. degree from Xidian University, Xi'an, China. He is currently the Chief Expert with China Electronics Technology Group Corporation. His research interests include telecommunication, RF circuits, antennas, and terahertz devices.

MINGJUN HU graduated from the Department of Materials Science and Engineering, City University of Hong Kong. He is currently an Associate Professor with Beihang University. His research interest includes flexible electronics, such as sensors, TFTs, and THz devices.
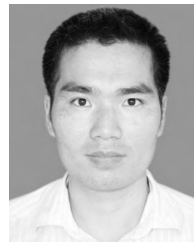
QIUQUAN GUO received the Ph.D. degree from Western University, where is currently a Research Associate with the Department of Mechanical and Materials Engineering. His research interests include micro/nano fabrication, MEMS technology, printed electronics, and sensors.

NAIBO ZHANG received the Ph.D. degree from the Beijing University of Posts and Telecommunications, Beijing, China, in 2012. From 2014 to 2016, he held a Postdoctoral position with Western University, Canada. His current research interests includes radio frequency (RF) devices, especially RF MEMS filters and terahertz filters.

JUN YANG received the Ph.D. degree from the University of Alberta, in 2004. He is currently a Professor with the Department of Mechanical and Materials Engineering, Western University. His research interests include micro/nano fabrication, MEMS/NEMS/BioMEMS, additive manufacturing/3D printing, printed electronics, metamaterials, flexible/wearable electronics, sensors, and surface engineering.

• • •